nature COMMUNICATIONS

ARTICLE

Received 18 Mar 2015 | Accepted 12 May 2015 | Published 25 Jun 2015

DOI: 10.1038/ncomms8475 OPEN

Large Seebeck effect by charge-mobility engineering

Peijie Sun[1], Beipei Wei[1], Jiahao Zhang[1], Jan M. Tomczak[2], A.M. Strydom[3,4], M. Søndergaard[5], Bo B. Iversen[5] & Frank Steglich[1,4]

The Seebeck effect describes the generation of an electric potential in a conducting solid exposed to a temperature gradient. In most cases, it is dominated by an energy-dependent electronic density of states at the Fermi level, in line with the prevalent efforts towards superior thermoelectrics through the engineering of electronic structure. Here we demonstrate an alternative source for the Seebeck effect based on charge-carrier relaxation: a charge mobility that changes rapidly with temperature can result in a sizeable addition to the Seebeck coefficient. This new Seebeck source is demonstrated explicitly for Ni-doped $CoSb_3$, where a marked mobility change occurs due to the crossover between two different charge-relaxation regimes. Our findings unveil the origin of pronounced features in the Seebeck coefficient of many other elusive materials characterized by a significant mobility mismatch. When utilized appropriately, this effect can also provide a novel route to the design of improved thermoelectric materials.

[1] Beijing National Laboratory for Condensed Matter Physics, Institute of Physics, Chinese Academy of Sciences, Beijing 100190, China. [2] Institute of Solid State Physics, Vienna University of Technology, A-1040 Vienna, Austria. [3] Highly Correlated Matter Research Group, Department of Physics, University of Johannesburg, Auckland Park 2006, South Africa. [4] Max Planck Institute for Chemical Physics of Solids, 01187 Dresden, Germany. [5] Department of Chemistry, University of Aarhus, DK-8000 Aarhus C, Denmark. Correspondence and requests for materials should be addressed to P.S. (email: pjsun@iphy.ac.cn).

Even though no fundamental constraints other than the Carnot efficiency are known to limit the potential efficiency of thermoelectric materials[1], the dimensionless figure of merit $ZT = T\,S^2\sigma/\kappa$ (T is the absolute temperature, S the Seebeck coefficient, σ the electrical conductivity and κ the thermal conductivity) in current materials hovers at values around 1, which are still inadequate for widespread applications[2,3]. Efforts to optimize ZT in general fall into two categories: 'phonon engineering' and 'electronic-structure engineering'. The most successful concept in this context is that of a phonon glass-electron crystal[4]. Here one attempts to reduce the thermal conductivity by incorporating intrinsic or extrinsic phonon scatterers while keeping the electronic properties unchanged[5]. Conversely, 'electronic-structure engineering'[1–3,6] pursues a favourable electronic dispersion at the Fermi level, ε_F, to achieve a higher thermoelectric power factor ($S^2\sigma$). Optimization of ZT through these concepts appears to be limited by the interdependence of the three relevant transport coefficients (S, σ and κ). In some specific systems, more exotic physical phenomena such as spin degeneracy and electronic correlations are also highly relevant to the Seebeck effect[7,8]; however, their impact is less transparent in practical material design.

The Seebeck coefficient of a conducting solid is generally induced by the asymmetry of the electronic density of states (DOSs) $N(\varepsilon)$ at the Fermi level ε_F, as illustrated in Fig. 1a. There, a temperature gradient ΔT_x along the sample leads to a slight gradient in the Fermi level ε_F (or, more generally, the chemical potential). Due to the energy dispersive $N(\varepsilon)$ and the Fermi function $f(\varepsilon)$, which both determine the charge-carrier density at ε_F, $n(\varepsilon_F) = N(\varepsilon_F)f(\varepsilon_F)$, a net diffusion of electrons occurs along the sample. The electron diffusion is eventually impeded by a retarding electric potential (V_x), leading to $S_N = V_x/|\Delta T_x|$ at equilibrium. We denote this conventional contribution to the Seebeck effect as S_N. From the thermodynamic point of view, this term measures the temperature derivative of ε_F per unit charge e, $S_N \propto (1/e)\,\partial\varepsilon_F/\partial T$. It also explains Seebeck's original observation of an electric potential across the junction of two metallic wires (cf. Fig. 1b). Here the difference of the Fermi energies of the two metals simply sets up an artificial energy dependence of $N(\varepsilon)$.

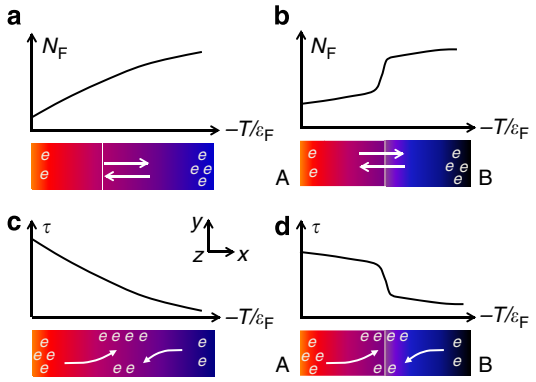

Figure 1 | The Seebeck effect derived from different asymmetries of charge carriers at the Fermi level. (**a**) A conducting solid with a significant energy-dependent DOSs. (**b**) A junction of conducting solids A and B with different DOSs, which is the situation where the Seebeck effect was originally discovered. (**c**) A conducting solid with a steep energy dependence of the electron relaxation time τ. (**d**) A junction between two conducting solids of significantly different τ. The vertical axis denotes either $N(\varepsilon)$ or $\tau(\varepsilon)$ at the Fermi level. The horizontal axis denotes temperature, or equivalently, the Fermi energy, due to their correlation. Note that scenarios **c** and **d** both produce a τ mismatch, which we exploit towards an enhanced Seebeck effect. When applying a magnetic field along the z direction, only in these two cases, transverse electric potential along the y direction (the Nernst effect) can be expected. In the case **a** and **b**, such a signal is fully compensated due to the Sondheimer cancellation (see text).

Here we demonstrate a new source for the Seebeck effect, S_τ, based on a charge mobility, $\mu_H(T)$, that changes rapidly with temperature. As illustrated in Fig. 1c, a large derivative $d\mu_H(T)/dT$ can generate a sizeable component S_τ adding to the conventional Seebeck coefficient S_N. As we shall see below, this scenario unifies the thermoelectric manifestations of various physical phenomena that lead to a significant gradient of charge-relaxation processes. The contribution S_τ can easily be distinguished from S_N by measuring the transverse thermoelectric signal (that is, the Nernst coefficient ν) in the presence of a magnetic field perpendicular to both S and ν. In materials with rapidly changing mobility, the Lorenz force affecting the slow and fast carriers of the cold and hot ends (or vice versa) will not fully compensate, leading to a sizeable value of ν that is dependent on S_τ (Fig. 1c). In cases with an insignificant thermal variation of $\mu_H(T)$ (Fig. 1a), the so-called Sondheimer cancellation removes the transverse potential since the Lorenz forces on the forward and backward flows of the electron current exactly compensate[9,10]. In analogy to the case shown in Fig. 1b, a proper engineering of the charge mobility, for example, by artificially fabricating a junction between the two conducting solids of very different mobilities, promises to further enhance the Seebeck effect, cf. Fig. 1d.

Results

Seebeck effect and charge mobility. The idea of using mobility gradients to enhance the Seebeck effect emerged from re-assessing the recent thermoelectric investigations on a specific material class of heavy fermions by two of the authors[11]. There an enhanced Seebeck coefficient was attributed to the asymmetric Kondo scattering processes of conduction electrons from localized $4f$ electrons. Characterizing the energy-dependent charge-relaxation time $\tau(\varepsilon)$ due to the Kondo effect, a significant Nernst coefficient $\nu(T)$ was observed and found to account for the enhanced Seebeck coefficient after renormalization by μ_H. This implies an inactivation of the Sondheimer cancellation, accounting for a sizeable $S_\tau \approx S$ in heavy fermions. Conceptually different from the local Kondo process, charge-relaxation time in a conventional solid is usually dominated by weakly energy-dependent scattering events, which, however, may exhibit a large temperature dependence due to, for example, a crossover between different relaxation regimes. As far as the thermal transport is concerned, an enhanced gradient of τ with respect to temperature is physically identical to an energy-dependent $\tau(\varepsilon)$ as evidenced by, for example, the Kondo effect. Notably, the former situation is much more transparent: regardless of the origin—we will discuss several possibilities below—sufficiently different charge mobilities at the hot and cold ends of a material will generate an electrical potential analogous to modifying the DOSs of an energy-dependent $N(\varepsilon)$ (cf. Fig. 1a,c).

Next, we will demonstrate the pivotal influence of the above mechanism for a weakly Ni-doped skutterudite $CoSb_3$. As shown in Fig. 2 (see also ref. 12), $S(T)$ of $Co_{0.999}Ni_{0.001}Sb_3$ is negative and only weakly temperature dependent above 50 K. Further cooling of the temperature leads to a marked sign change of $S(T)$ and a pronounced positive peak of $110\,\mu V\,K^{-1}$ at $T \approx 20$ K. Here we highlight the opposite signs of $S(T)$ and $R_H(T)$ below 30 K, the latter being negative in the whole temperature range investigated (cf. Fig. 3a). Phonon-drag effects are unlikely to play the key role

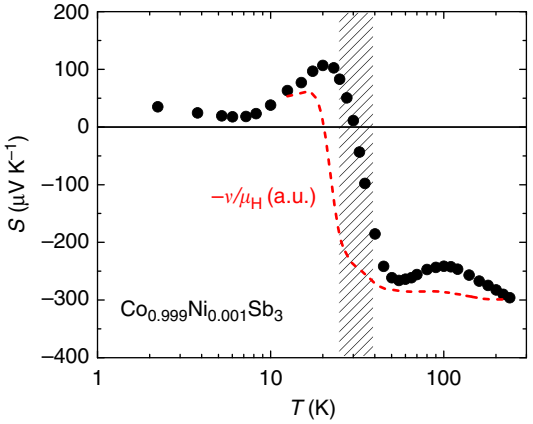

Figure 2 | The Seebeck coefficient $S(T)$ of $Co_{0.999}Ni_{0.001}Sb_3$. The measured $S(T)$ is compared with calculated values of $-\nu/\mu_H$, that is, the expected Seebeck contribution, S_τ, derived from the mobility gradient, see text. Note that the positive peak developed below 50 K due to the *n*-type charge carriers can be well reproduced by this ratio. The hatched area indicates the temperature window where two electron-like bands are involved, and these cannot describe the occurrence of the positive $S(T)$ peak.

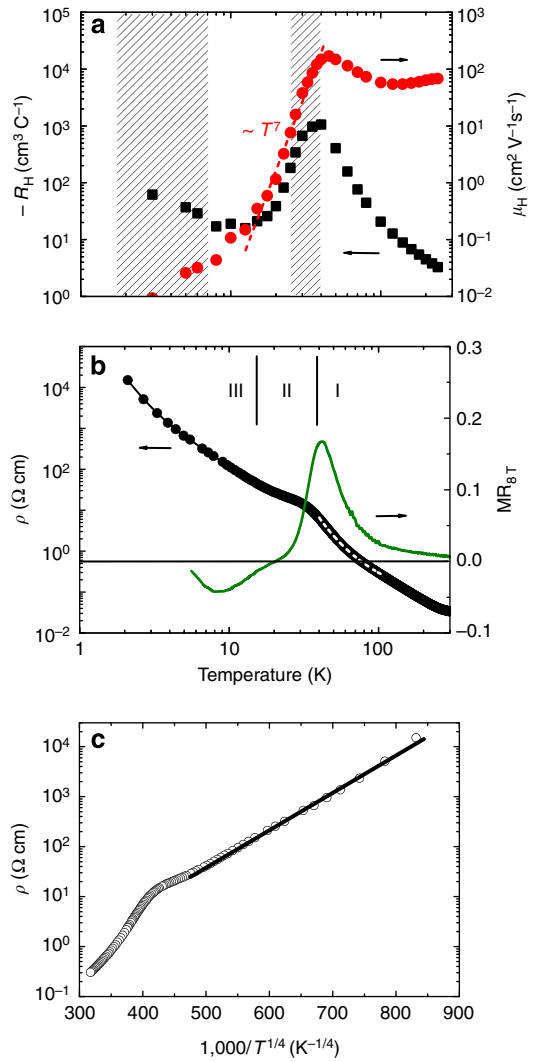

Figure 3 | Electrical transport properties of $Co_{0.999}Ni_{0.001}Sb_3$. (**a**) Hall coefficient $R_H(T)$ and Hall mobility $\mu_H(T)$, defined as $|R_H(T)|/\rho(T)$. The dashed line indicates an approximate T^7 dependence of $\mu_H(T)$. The hatchings indicate the regions where multiband effects are present. The one at around 30 K involves two electron-like bands and the one below 7 K is complex and beyond the scope of this work. (**b**) Electrical resistivity $\rho(T)$ and magnetoresistance $MR(T) = [\rho_B(T) - \rho_0]/\rho_0$. The latter quantity was measured in a magnetic field $B = 8$ T. Three different regions (I, II and III) are indicated, of which region I is characterized by high mobility, intrinsic or deeper donor-derived conductance and region III by low-mobility variable range hopping. The dashed line on top of the $\rho(T)$ curve represents a fit by the thermal activation law. (**c**) Electrical resistivity plotted as log ρ versus $T^{-1/4}$. A linear dependence, as well as the negative MR(T) below about 15 K is characteristic of VRH conduction. VRH, variable range hopping.

in the origin of the extraordinary $S(T)$ peak at 20 K due to its absence in undoped $CoSb_3$ and its sensitivity to slight change in Ni concentration[12]. In view of the opposite signs of $S(T)$ and $R_H(T)$ and to account for the unusual peak in the former, an intuitive approach involves a two-band model, with charge carriers of different signs being involved. This is, however, in contradiction to the Hall resistivity data that hint to two electron-like bands (cf. Supplementary Fig. 1 and Supplementary Note 1), whose influences furthermore only coexist in a very limited temperature region (25 − 40 K, hatched in Fig. 2). Near 20 K, the one-band nature is restored. These observations imply that, while two-band effects are involved in a limited temperature interval (cf. Figs 2 and 3a), they are not responsible for the positive $S(T)$ peak. Another likely multiband regime below $T \approx 7$ K (cf. Fig. 3a) is beyond the scope of this investigation. In view of the sublinear $\rho_H(B)$ above 10 K, we proceed our discussion in the framework of a one-band picture. This applies at least to the low magnetic field region ($B \leq 2$ T) where we have measured $\nu(T)$ and estimated $R_H(T)$.

The occurrence of a peak in $R_H(T)$ and a shoulder in $\rho(T)$ at $T \approx 40$ K (cf. Fig. 3a,b) supports the notion of an electron-like shallow impurity level that becomes active below 40 K, due to the surplus electrons of Ni atoms. Applying the thermal activation law $\rho = \rho_0 \exp(E_a/k_B T)$ to the T range 40 − 110 K above the shoulder (region I, Fig. 3b), the activation energy E_a is estimated to be 207 K. This is associated with either an intrinsic electronic band or a deeper donor level[12]: as revealed in Fig. 3a, these states are characterized by a high charge mobility. Due to the narrow temperature window, we have not estimated the activation energy for region II (15 − 40 K). Instead, we stress that the data below ~15 K (region III) can be well described by the variable range hopping model, expected for conducting states of weak localization. The observation of negative values of magnetoresistance and a characteristic dependence of log $\rho \sim (1/T)^{1/4}$ in regime III lend strong support to this proposition (Fig. 3b,c; ref. 12). Consequently, a pronounced change of $\mu_H(T)$ connecting a region with high-mobility (intrinsic or deepe donor derived) charge carriers to a low-mobility variable range hopping conduction occurs due to the onset of a shallow impurity level. The pronounced change of the mobility, following $\mu_H(T) \sim T^7$ between 40 and 10 K (Fig. 3a), dwarfs the characteristics of common charge scattering processes, for example, the $T^{3/2}$ dependence expected for ionized impurity scattering.

Nernst effect. What are the consequences for the Nernst response? In a nonmagnetic, non-superconducting one-band system[9,13],

$$\nu = -\frac{\pi^2}{3}\frac{k_B^2 T}{B|e|}\frac{\partial \tan\theta_H}{\partial \varepsilon}\Big|_{\varepsilon=\varepsilon_F} \quad (1)$$

Here the energy derivative of the tangent of the Hall angle can be

expressed by using either μ_H or τ because $\tan\theta_H = eB\tau/m^* = \mu_H B$, where m^* denotes the effective mass of the relevant charge carriers. Apparently, ν is sensitive to any charge-relaxation process that is asymmetric with respect to ε. However, the asymmetry associated with ordinary scattering events is typically rather weak, and representable by a power-law dependence of $\tau(\varepsilon) \sim \varepsilon^r$ with $|r| \approx 1$ for, for example, electron scattering by acoustic phonons. Replacing $1/\partial\varepsilon$ in equation (1) by $1/k_B\partial T$, one immediately recognizes that an enhanced gradient of μ_H with respect to T similarly can supply a finite Nernst coefficient $\nu = AT\mathrm{d}\mu_H/\mathrm{d}T$, where $A = -(\pi^2/3)\ k_B/|e|$. As can be seen in Fig. 4, the pronounced $\nu(T)$ peak observed slightly below 40 K for $Co_{0.999}Ni_{0.001}Sb_3$ follows this prediction quantitatively, underlining the existence of distinctly different charge mobilities at the two ends of the sample when exposed to a temperature gradient (cf. Figs 1c and 3a). Given that above 40 K $\mu_H(T)$ is only weakly dependent on temperature, one expects $\nu(T) \propto \mu_H(T)$ ($\mathrm{d}\mu_H/\mathrm{d}T$ is approximated to first order as μ_H/T, cf. ref. 9). This is also confirmed in Fig. 4 and at $T > 40$ K, $\nu(T)$ scales well with $\mu_H(T)$ (red dashed line).

Discussion

We now scrutinize how the large mobility gradient impacts upon the Seebeck effect. The Mott expression relates the Seebeck coefficient to the logarithmic energy derivatives of $N(\varepsilon)$ and $\tau(\varepsilon)$ at the Fermi energy,

$$S = -\frac{\pi^2}{3}\frac{k_B^2 T}{e}\left[\frac{\partial \ln \tau}{\partial \varepsilon} + \frac{\partial \ln N}{\partial \varepsilon}\right]_{\varepsilon_F} = S_\tau + S_N. \qquad (2)$$

Even though S_τ due to asymmetric charge relaxation has been ignored in most thermoelectric explorations, it can in fact be the dominating term in specific cases such as heavy-fermion systems, as was realized recently [11]. As discussed in Supplementary Note 2 and refs 10,11, the Nernst coefficient is physically linked to S_τ by $\nu \cdot B = \pm S_\tau \tan\theta_H$ (or, $\nu = \pm S_\tau\ \mu_H$), since $\tan\theta_H \propto \tau$ in a conventional one-band solid. An additional $S_\tau = -\nu/\mu_H$ is, therefore, expected to occur in $Co_{0.999}Ni_{0.001}Sb_3$ due to the abrupt mobility change. Here the negative sign refers to the electron-like charge carriers. Remarkably, the ratio $-\nu/\mu_H$ can indeed account for the abrupt crossover and the positive $S(T)$ peak emerging below 50 K (dashed line in Fig. 2). This offers compelling evidence that the rapidly changing mobility is underlying this extraordinary thermoelectric response.

To substantiate this assessment also from the theoretical point of view, we have computed the Seebeck coefficient based on state-of-the-art one-particle electronic-structure calculations, assuming a constant scattering rate τ. While by construction missing out on the mobility-driven effects, this procedure is expected to qualitatively capture all intrinsic DOSs effects, and therewith in particular the contribution S_N to the Seebeck coefficient. This expectation is indeed fulfilled: The theoretical S_N of $Co_{0.999}Ni_{0.001}Sb_3$, which is negative for all temperatures, approaches the experimental result at only high temperatures, where S_τ is expected to be less relevant (cf. Supplementary Fig. 2 and Supplementary Note 3).

In view of both the very similar $\mu_H(T)$ profiles and the competing signs of $S(T)$ and $R_H(T)$ at low temperatures, the scenario described above will be able to explain the positive peak in $S(T)$ observed also for other doping levels of $Co_{1-x}Ni_xCo_3$ reported in ref. 12. One may notice that, in the nominally pure $CoSb_3$, a similar mobility gradient exists with, however, $R_H(T)$ being positive. The opposite sign of the charge carriers in pure $CoSb_3$ relative to that of the Ni-doped $CoSb_3$ will naturally invert the sign of the corresponding S_τ. This may account for the abrupt drop of $S(T)$ in $CoSb_3$ from positive to small negative values below $c.100$ K (cf. Fig. 5 of ref. 12).

In Table 1, we summarize the expected signs for the mobility-driven Seebeck effect (S_τ) and the Nernst coefficient (ν) based on equations (1) and (2). The signs are solely determined by the direction of the mobility gradient and the type of the charge carriers. Clearly, a negative $\mathrm{d}\mu_H/\mathrm{d}T$ is technically more attractive since in this case, a positive (negative) S_τ would add to a p-type (n-type) transport, leading to an overall enhancement of the Seebeck coefficient.

The significance of our findings is straightforward, yet wide-ranging: an additional Seebeck coefficient S_τ is generated whenever a temperature-dependent μ_H exists. However, since $S_\tau = \pm\nu/\mu_H$, the mobility-driven Seebeck effect will be sizeable or even dominating only if the gradient $\mathrm{d}\mu_H/\mathrm{d}T$ is huge, but not μ_H itself. This concept is far more general than what has been discussed for heavy fermions based on the Kondo effect. We can think of a variety of materials whose thermoelectric responses conform to our unifying scenario: for example, in Cu_2Se, a structural phase transition occurs at $\sim$400 K, where μ_H changes abruptly with temperature due to critical scattering. Correspondingly, an unconventional Seebeck coefficient contributing largely to the enhanced ZT values has indeed been observed and attributed to abnormal scattering processes concomitant to the

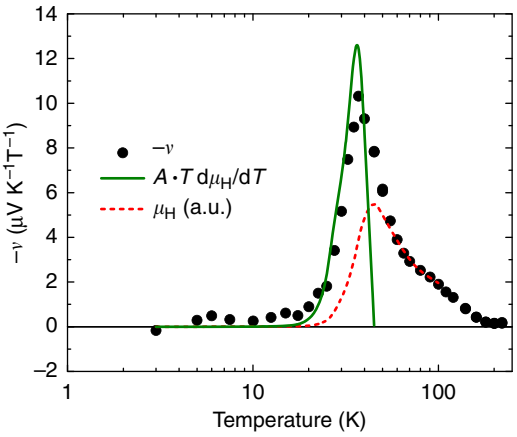

Figure 4 | The Nernst coefficient of $Co_{0.999}Ni_{0.001}Sb_3$. The green solid line represents $AT\mathrm{d}\mu_H/\mathrm{d}T$, the expected contribution to $\nu(T)$ from the marked charge mobility change (cf. equation (1)), where the prefactor $A = -(\pi^2/3)\ k_B/|e|$. The quantitative agreement found below 40 K between this calculation and the measured Nernst coefficient (black symbols) lends strong evidence that the enhanced Nernst signal originates from the significant mobility mismatch across the sample. The red dashed line displays the Hall mobility $\mu_H(T)$. $\nu(T)$ is expected to approximately scale with $\mu_H(T)$ assuming a weak temperature dependence of the latter, which indeed holds above 40 K (see text for details).

Table 1 | The expected sign of the mobility-driven Nernst coefficient ν and Seebeck effect S_τ for the different combinations of the signs of both the charge carrier and $\mathrm{d}\mu_H/\mathrm{d}T$.

$\mathrm{d}\mu_H/\mathrm{d}T$	Charge carrier	
	Hole	Electron
+	ν (−); S_τ (−)	ν (−); S_τ (+)
−	ν (+); S_τ (+)	ν (+); S_τ (−)

The symbols + and − denote positive and negative values, respectively.

phase transition[14]. Importantly, the sign of the additional Seebeck coefficient indeed follows our prediction shown in Table 1. Another example that deserves attention is $AgBiSe_2$ (ref. 15), which develops a large negative $S(T)$ maximum out of p-type transport at around 580 K. This feature concurs with a pronounced change of the electrical conductivity, where a marked change of the mobility is expected. It is, therefore, highly desirable to see whether the current scenario can apply. Our scenario appears to be active also in the recently discovered heavy-fermion compound $CeRu_2Al_{10}$ (ref. 16), where a sharp negative gradient of $\mu_H(T)$ is found at $T \approx 20$ K, along with an anomalous $S(T)$ peak (cf. Supplementary Figs 3 and 4). These observations can indeed be described within the current framework, as discussed in Supplementary Note 4. More examples may be expected/found in compounds where a phase transition or crossover between two regimes of significantly different charge-relaxation mechanisms, for example, associated with Mott or Anderson localization, takes place. One may also envision engineering the charge mobility of a heterogeneous semiconductor along a certain direction by, for example, controlled doping. Alternatively, one could fabricate an artificial junction from two, preferably already functionally well-graded, thermoelectric materials with very different mobilities to further improve the performance. By disentangling the impact of the gradients of the one-particle DOSs and the charge mobility (or life time) onto thermoelectricity, our findings will also help answering fundamental questions in more complex systems. This pertains in particular to electron-correlated materials, in which the two gradients are convoluted in the many-body spectral function. Further investigations to explore, as well as exploit, the overarching framework of mobility gradients are eagerly called for, both from the fundamental and technological points of view.

Methods

Sample synthesis and characterization. The sample of $Co_{0.999}Ni_{0.001}Sb_3$ employed in this work was synthesized by two steps. First, stoichiometric amounts of high purity starting materials were melted in an induction furnace at a temperature of 1,400 °C. This procedure yields material of a fine powder morphology, which has been checked by X-ray diffraction to be single phase. Then, the powder was compacted with a spark plasma sintering technique under a pressure of 40 MPa, by heating to 630 °C in 6 min and keeping at that temperature for 5 min. The purity of the finally obtained sample was checked again by powder X-ray diffraction (cf. Supplementary Fig. 5). The high purity and crystalline quality of the current sample are further evidenced by the fact that its electrical resistivity $\rho(T)$ is enhanced by nearly six orders of magnitude with decreasing temperature from 300 to 2 K (cf. Fig. 3b in the main text). This enhancement of $\rho(T)$ is more than one order of magnitude larger than that reported in ref. 12.

Transport measurements. The Nernst and Seebeck coefficients (ν and S) were measured between 2 K and room temperature using a conventional static heater-and-sink method. A chip resistor (2,000 Ω) was used as heater and one thin ($\varphi = 25$ μm) chromel-AuFe 0.07% thermocouple was employed to detect the temperature gradient. The values of S and ν were determined following the respective definitions $S = E_x/|\Delta T_x|$ and $\nu = E_y/B_z|\Delta T_x|$, with ΔT_x being the applied temperature gradient, $B_z = 2$ T the magnetic field and E_x (E_y) the induced electrical potential along the x (y) direction (cf. Fig. 1). For detecting E_x and E_y, Keithley 2,182 nanovoltmeters were employed. Here we adopt the convention that the sign of the Seebeck coefficient represents the potential of the cold side with respect to the hot side, and the sign of Nernst coefficient follows the historical convention as used in thermoelectric investigations[9]. In addition, electrical resistivity, $\rho(T)$, and Hall coefficient, $R_H(T)$, were also measured to facilitate our analysis, with a conventional four-probe technique using a Physical Property Measurement System (PPMS, Quantum Design). A sample of typical dimension $0.5 \times 2 \times 5$ mm^3 was used for all the transport measurements. The measurements of Nernst and Hall effect were performed in magnetic fields of opposite directions to eliminate the Seebeck and resistive contribution, respectively.

References

1. Mahan, G. D. & Sofo, J. O. The best thermoelectric. *Proc. Natl Acad. Sci. USA* **93,** 7436–7439 (1996).
2. Sootsman, J. R., Chung, D. Y. & Kanatzidis, M. G. New and old concepts in thermoelectric materials. *Angew. Chem. Int. Ed. Engl.* **48,** 8616–8639 (2009).
3. Snyder, G. J. & Toberer, E. S. Complex thermoelectric materials. *Nat. Mater.* **7,** 105–114 (2008).
4. Slack, G. A. in *CRC Handbook of Thermoelectrics*. (ed Rowe, D. M.) Ch. 34 (CRC, 1995).
5. Sales, B. C., Mandrus, D. & Williams, R. K. Filled skutterudite antimonides: a new class of thermoelectric materials. *Science* **272,** 1325–1328 (1996).
6. Heremans, J. P. *et al.* Enhancement of thermoelectric efficiency in PbTe by distortion of the electronic density of states. *Science* **321,** 554–557 (2008).
7. Terasaki, I., Sasago, Y. & Uchinokura, H. Large thermoelectric power in $NaCo_2O_4$ single crystals. *Phys. Rev. B* **56,** 12685–12687 (1997).
8. Zlatić, V. *et al.* Thermoelectric power of cerium and ytterbium intermetallics. *Phys. Rev. B* **68,** 104432 (2003).
9. Behnia, K. The Nernst effect and the boundaries of the Fermi liquid picture. *J. Phys. Condens. Matter* **21,** 113101 (2009).
10. Wang, Y. *et al.* Onset of the vortexlike Nernst signal above T_c in $La_{2-x}Sr_xCuO_4$ and $Bi_2Sr_{2-y}La_yCuO_6$. *Phys. Rev. B* **64,** 224519 (2001).
11. Sun, P. & Steglich, F. Nernst effect: Evidence of local Kondo scattering in heavy fermions. *Phys. Rev. Lett.* **110,** 216408 (2013).
12. Dyck, J. S., Chen, W., Yang, J., Meisner, G. P. & Uher, C. Effect of Ni on the transport and magnetic properties of $Co_{1-x}Ni_xSb_3$. *Phys. Rev. B* **65,** 115204 (2002).
13. Sondheimer, E. H. The theory of the galvanomagnetic and thermomagnetic effects in metals. *Proc. Roy. Soc. London* **193,** 484–512 (1948).
14. Liu, H. *et al.* Ultrahigh thermoelectric performance by electron and phonon critical scattering in $Cu_2Se_{1-x}I_x$. *Adv. Mater.* **25,** 6607–6612 (2013).
15. Xiao, C. *et al.* High thermoelectric and reversible *p-n-p* conduction type switching integrated in dimetal chalcogenide. *J. Am. Chem. Soc.* **134,** 18460–18466 (2012).
16. Strydom, A. M. Thermal and electronic transport in $CeRu_2Al_{10}$: Evidence for a metal-insulator transition. *Phys. B* **404,** 2981–2984 (2009).

Acknowledgements

We thank J.L. Snyman for valuable assistance with materials synthesis, and N.L. Wang, J.L. Luo, Y.F. Yang, Q. Si, H.Z. Zhao, M. Baenitz, J. Grin, and G. Kotliar for discussions. P.S., B.W. and J.Z. are thankful to the financial support from the MOST of China (Grant Nos: 2012CB921701 and 2015CB921303), the National Science Foundation of China (Grant No: 11474332), and the Chinese Academy of Sciences through the strategic priority research program (Grant No: XDB07020200). A.M.S. thanks the SA-NRF (93549) and the FRC/URC of UJ for financial assistance, and the IOP-CAS for a visiting professor fellowship. J.M.T. thanks COST Action MP1306 EUSpec for support. M.S. and B.B.I. thank the Danish National Research Foundation (DNRF93) for support.

Author contributions

P.S. and F.S. conceived the idea. P.S., B.W. and J.Z. performed all the electrical and thermal transport experiments and analysed the data, after discussion with other authors. J.M.T performed the electronic-structure and thermoelectric calculations. A.M.S., M.S. and B.B.I. prepared the sample and carried out sample characterization. P.S. and F.S. wrote the manuscript and all authors commented on and edited the manuscript.

Additional information

Supplementary Information accompanies this paper at http://www.nature.com/naturecommunications

Competing financial interests: The authors declare no competing financial interests.

Reprints and permission information is available online at http://npg.nature.com/reprintsandpermissions/

How to cite this article: Sun, P. *et al.* Large seebeck effect by charge-mobility engineering. *Nat. Commun.* 6:7475 doi: 10.1038/ncomms8475 (2015).